

## EFFECTS OF NON-THERMAL ELECTRONS AND NON-EXTENSIVE POSITRONS ON SOLITARY WAVES IN A MULTI-COMPONENT DUSTY PLASMA

 Satyendra Nath Barman<sup>1</sup>,  Kingkar Talukdar<sup>2\*</sup>

<sup>1</sup>B. Borooah College, Guwahati 781007, Assam, India

<sup>2</sup>Department of Mathematics, Gauhati University, Guwahati 781014, Assam, India

\*Corresponding Author email [kingkartalukdar5@gmail.com](mailto:kingkartalukdar5@gmail.com)

Received March 2, 2026; Revised April 15, 2026; Accepted May 13, 2026

In this study, we have investigated the existence and characteristics of solitons in an unmagnetized dusty plasma composed of cold ions, negatively charged dust grains, positively charged dust grains, non-thermal electrons, and non-extensive positrons. The properties of solitons are usually studied through the Reductive Perturbation method and the Sagdeev Potential method. We have derived the energy integral equation using the Sagdeev Potential method. We have also discussed the variation of the Sagdeev potential for different values of the parameters involved in our plasma model. The non-extensive parameter ( $q$ ), the non-thermal parameter ( $\beta$ ), charge density ratio of positively charged dust ( $\delta_+$ ), charge density ratio of negatively charged dust ( $\delta_-$ ), positron to ion density ratio ( $\delta_p$ ), electron to ion density ratio ( $\delta_e$ ), electron to positron temperature ratio ( $\sigma_p$ ) and the Mach number ( $M$ ) found to influence the amplitude of solitons. Our study reveals that non-thermality of electrons and non-extensivity of positrons significantly modify the soliton features. The results from our study can be useful for investigating plasma in space environments such as cometary tails and interstellar clouds.

**Keywords:** *Non-thermal; Solitary waves; Sagdeev potential; Energy integral; Dusty plasma*

**PACS:** 95.30.Qd, 05.45.Yv, 52.35.Fp, 05.10.-a, 52.35.Mw

### 1. INTRODUCTION

Unmagnetized plasma is vital in studying astrophysical phenomena, such as solar winds, cometary tails, interstellar clouds and also in industrial applications like plasma processing, etching, and coating. Several studies have been conducted on unmagnetized plasma in recent years [1-17]. The presence of dust grains in unmagnetized plasma transforms it from a simple ionized gas into a complex plasma. In unmagnetized state, the physics is driven entirely by the local electric environment and the inertia of the dust, rather than being forced along magnetic field lines. Dust grains in plasma are essential for understanding astrophysical phenomena, including the formation of celestial bodies in protoplanetary disks, the structure of planetary rings (e.g., Saturn's rings), and also the behaviour in comet tails. Dust particles in plasma transform standard electron-ion plasma into a complex system that acts as a model for atomic structures, creating plasma crystals. Presence of dust grains can affect the soliton amplitude and Mach number for both compressive and rarefactive solitons [18]. In some plasma model presence of positively charged dust grains results in existence of compressive solitons; however, the presence of negatively charged dust grains results in compressive solitons only up to a certain concentration of dust, and above the critical concentration of negative charge, the dusty plasma supports rarefactive solitons [19]. The effect of variable dust charge, dust temperature and trapped electrons on small-amplitude dust acoustic waves is investigated in [20]. The presence of dust charge of immobile dust plays crucial role to form compressive and rarefactive solitons in plasma where the massive dust particles are in the stationary background of the plasma, and the lighter ions and relativistic electrons get appreciable initial drifts which makes great change in the growth of solitons [21]. The Dust-Ion-Acoustic (DIA) solitary waves are highly sensitive to the ion streaming speed and their amplitude decreases with an increase of the ion streaming speed [22]. In the presence of low dust charges and lower ion streaming, compressive and rarefactive solitons of either concave or convex characters reflect. The higher streaming of mobile dusts causes the amplitudes of rarefactive solitons characteristically change from higher to lower, showing convex character [23]. Dust grain density enhances the amplitude of solitary waves but weakens their reflection. In which, the amplitudes of both the incident and reflected solitons remain higher for fluctuating charge on the dust grains in comparison with the case of fixed charge [24]. In plasma physics, researchers often assume particles to follow a Maxwellian distribution; however, real-world plasmas often contain nonthermal electrons. These nonthermal electrons are high-energy particles that exist in the tail of the distribution. In unmagnetized plasmas, there is no external magnetic field to constrain particle motion, which indicates that non-thermal electrons are critical in unmagnetized plasma as they dominate the transport of energy and the stability of the system. The non-thermal electrons in unmagnetized plasma significantly alters the formation, behaviour, and structural characteristics of nonlinear waves and electrostatic structures, often departing from standard Maxwellian behaviour to model realistic space and laboratory scenarios. Large amplitude solitary structures significantly depend on various plasma parameters such as ion drift velocity, non-thermal parameter, electron to positron temperature ratio, positron density, and Mach number [25]. The presence of non-thermal electrons significantly modifies the parametric region where electron acoustic solitons can exist [26]. In some plasma model, increase of nonthermal parameter decreases the peak amplitude of solitons [27]. The solitary excitations also strongly depend on the mass and density ratios of the

positive and negative ions as well as the nonthermal electron parameter [28]. When the non-thermality of hot electrons rises, the speed of electron beam decreases, the density ratio of the beam to the cold electron increases, and the existence domain for electron acoustics solitons gets bigger [29]. The presence of non-thermal electrons also significantly affects the existence of super solitons [30]. Increase in the non-thermal electron effects based on a Cairns (kappa) distribution has the effect of reducing (increasing) the width of the stopband [31]. Non-extensive positrons in unmagnetized plasma are important as they more accurately model particle distributions in systems characterized by long-range correlations and non-equilibrium states, where standard Maxwellian distributions fail. These non-extensive distributions, often described by the q-nonextensive or Tsallis statistics, significantly modify the fundamental characteristics of nonlinear waves. These non-extensive distributions also provide efficient modelling for observed particle populations in scenarios such as solar winds, planetary rings, cometary tails, and galactic clusters. Different values of the non-extensive parameter q show significant effect on chaotic motions of ion acoustic waves [32]. Ion-acoustic solitary wave can also depend on non-extensive parameter, electron to positron temperature ratio, ion to electron temperature ratio and streaming velocity. Fast ion-acoustic modes solely can produce the coexistence of small amplitude rarefactive solitons [33]. Particle non-extensivity can affect the properties of nonplanar ion-acoustic rarefactive and compressive solitons [34]. The non-extensive parameter, positron-to-electron density ratio, ion-to-electron temperature ratio, electron-to-positron temperature ratio and relativistic factor can significantly influence the phase shifts of solitary waves [35]. While solitons have been studied in various plasma configurations, their characteristics in a system featuring both positively and negatively charged dust grains, cold ions alongside non-extensive positrons and nonthermal electrons remain underexplored.

In this paper, we have represented the introduction in Section 1. The fluid equations (that govern our plasma model) and the standard energy integral equation is represented in section 2. Effects of several parameters on the characteristics of solitons are discussed in Section 3. Finally, we have concluded our research in Section 4.

## 2. EQUATIONS GOVERNING DYNAMICS OF PLASMA

We consider an unmagnetized plasma model composed of cold ions, positively charged dust grains, negatively charged dust grains, non-thermal electrons and non-extensive positrons. The equations governing dynamics of plasma are as follows:

For cold ions

$$\frac{\partial n_i}{\partial t} + \frac{\partial}{\partial x}(n_i u_i) = 0, \tag{1}$$

$$\frac{\partial u_i}{\partial t} + u_i \frac{\partial u_i}{\partial x} = -\frac{\partial \phi}{\partial x}. \tag{2}$$

For positively charged dust grains,

$$\frac{\partial n_{d+}}{\partial t} + \frac{\partial}{\partial x}(n_{d+} u_{d+}) = 0, \tag{3}$$

$$\frac{\partial u_{d+}}{\partial t} + u_{d+} \frac{\partial u_{d+}}{\partial x} = -\mu_{d+} \frac{\partial \phi}{\partial x}. \tag{4}$$

For negatively charged dust grains,

$$\frac{\partial n_{d-}}{\partial t} + \frac{\partial}{\partial x}(n_{d-} u_{d-}) = 0, \tag{5}$$

$$\frac{\partial u_{d-}}{\partial t} + u_{d-} \frac{\partial u_{d-}}{\partial x} = \mu_{d-} \frac{\partial \phi}{\partial x}. \tag{6}$$

Here,  $\mu_{d+} = \frac{Z_{d+} m_i}{m_{d+}}$  and  $\mu_{d-} = \frac{Z_{d-} m_i}{m_{d-}}$ , where  $Z_{d+}$  and  $Z_{d-}$  are positive and negative dust charge number respectively, and  $m_i$ ,  $m_{d+}$  and  $m_{d-}$  are the mass of ion, mass of positively charged dust grain and mass of negatively charged dust grain respectively.

Following the procedure in [36], the non-thermal electron's number density is obtained over velocity space with dimensionless potential  $\phi$  as,

$$n_e = (1 - \beta\phi + \beta\phi^2)e^{\phi}. \tag{7}$$

Here,  $\beta = \frac{4\alpha}{1+3\alpha}$  represents the non-thermality, where  $\alpha$  determines the non-thermal electrons in the non-thermal plasma model. The parameter  $\alpha$  determines the population of dynamic nonthermal electrons in the nonthermal plasma model. In many space and laboratory plasmas, the distribution of particles does not follow the usual Boltzmann–Gibbs statistics which is an efficient tool for investigating the system when the memories and microscopic interactions are short ranged. The generalization of Boltzmann–Gibbs–Shannon (BGS) entropy for statistical equilibrium with long-range interactions, long-time memories, and dissipation is noted by Renyi [38] and Tsallis [39]. For two independent systems  $\alpha$  and  $\beta$  the rule of composition can be written as  $S_q(\alpha + \beta) = S_q(\alpha) + S_q(\beta) + (1 - q)S_q(\alpha)S_q(\beta)$ ,  $q \neq 1$  where the parameters show the grade of correlation of the system under consideration.

The non-extensive distribution function for positrons can be obtained as,

$$f_p(q) = C_q \left[ 1 - (q-1) \left( \frac{m_p u^2}{k_B T_p} + \frac{Q_p \Phi}{k_B T_p} \right) \right]^{\frac{1}{q-1}}.$$

Where:

$$C_q = \frac{n_{p0} \Gamma\left(\frac{1}{1-q}\right)}{\Gamma\left(\frac{1}{1-q} + \frac{1}{2}\right)} \sqrt{\frac{m_p(1-q)}{2\pi T_p}}, \quad -1 < q < 1, \text{ and, } C_q = n_{p0} \left(\frac{1+q}{2}\right) \frac{\Gamma\left(\frac{1}{1-q} + \frac{1}{2}\right)}{\Gamma\left(\frac{1}{1-q}\right)} \sqrt{\frac{m_p(1-q)}{2\pi T_p}}, \quad q > 1.$$

Where,  $C_q$  is the normalization constant and  $\Gamma$  represents gamma function. The normalized positron number density can be given by [40],

$$n_p = (1 - (q-1)\sigma_p \Phi)^{\frac{q+1}{2(q-1)}}. \quad (8)$$

Equation (8) can be written as

$$n_p = 1 - \sigma_p \frac{(q+1)}{2} \Phi. \quad (9)$$

Where,  $\sigma_p = \frac{T_e}{T_p}$  is the electron to positron temperature ratio and  $q$  represents the non-extensive strength. Extensivity, sub extensivity and super extensivity are represented by  $q=1$ ,  $q>1$  and  $q < 1$  respectively.

The normalized Poisson equation can be written as,

$$\frac{\partial^2 \Phi}{\partial x^2} = \delta_e n_e - \delta_p n_p + \delta_- n_{d-} - \delta_+ n_{d+} - n_i. \quad (10)$$

The Charge neutrality condition is,  $\delta_e + \delta_- = 1 + \delta_+ + \delta_p$

Here,  $\delta_e = \frac{n_{e0}}{n_{i0}}$ ,  $\delta_p = \frac{n_{p0}}{n_{i0}}$  are the equilibrium electron-to-ion density ratio and the equilibrium positron-to-ion density ratio respectively. Also,  $\delta_+ = \frac{Z_{d+} n_{d+0}}{n_{i0}}$  and  $\delta_- = \frac{Z_{d-} n_{d-0}}{n_{i0}}$  are the equilibrium charge density ratio of positively charged dust and negatively charged dust respectively. The number density of ions, positively charged dust grains, negatively charged dust grains, non-thermal electrons and non-extensive positrons are represented by  $n_i$ ,  $n_{d+}$ ,  $n_{d-}$ ,  $n_e$  and  $n_p$  respectively. The number densities are normalized by the equilibrium density of ion  $n_{i0}$ .

The fluid velocity of ion, positively charged dust grains and negatively charged dust grains are represented by  $u_i$ ,  $u_{d+}$  and  $u_{d-}$  respectively, which are normalized by the ion acoustic speed  $c_i = \sqrt{\frac{k_B T_e}{m_i}}$  and the electrostatic potential  $\Phi$  is normalized by  $\frac{k_B T_e}{e}$ , where,  $T_e$ ,  $k_B$ ,  $m_i$  and  $e$  represents electron temperature, Boltzmann's constant, ion mass and electronic charge respectively. The time and space variables are normalized by the inverse of the ion plasma frequency  $\omega_{pi}^{-1} = \sqrt{\frac{m_i}{4\pi e^2 n_{i0}}}$  and Debye length  $\lambda_D = \sqrt{\frac{k_B T_e}{4\pi e^2 n_{i0}}}$  respectively.

We consider a variable  $\xi = x - Mt$  (where,  $M$  represents the Mach number), that influences all the dependent variables in the nonlinear equations to employ the Sagdeev potential (pseudopotential) method.

Applying the boundary conditions  $\xi \rightarrow \pm\infty$ ,  $n_i \rightarrow 1$ ,  $n_{d+} \rightarrow 1$ ,  $n_{d-} \rightarrow 1$ ,  $u_i \rightarrow 0$ ,  $u_{d+} \rightarrow 0$ ,  $u_{d-} \rightarrow 0$ ,  $\Phi \rightarrow 0$ , we obtain the overall solution for  $n_i$ ,  $n_{d+}$  and  $n_{d-}$  as,

$$n_i = \left( 1 - \frac{2\Phi}{M^2} \right)^{-\frac{1}{2}}, \quad (11)$$

$$n_{d+} = \left( 1 - \frac{2\mu_{d+}\Phi}{M^2} \right)^{-\frac{1}{2}}, \quad (12)$$

$$n_{d-} = \left( 1 + \frac{2\mu_{d-}\Phi}{M^2} \right)^{-\frac{1}{2}}. \quad (13)$$

Applying the fundamental densities from the equations (7), (9), (11), (12) and (13) into the equation (10) and then multiplying  $\frac{d\Phi}{d\xi}$ , we get the standard energy integral equation as,

$$\frac{1}{2} \left( \frac{d\Phi}{d\xi} \right)^2 + V(\Phi) = 0. \quad (14)$$

Here,  $V(\Phi)$  represents the Sagdeev Potential in the energy integral equation (14). The  $V(\Phi)$  is given by,

$$V(\Phi) = -M^2 \left[ \sqrt{1 - \frac{2\Phi}{M^2}} - 1 \right] - \frac{\delta_+ M^2}{\mu_{d+}} \left[ \sqrt{1 - \frac{2\mu_{d+}\Phi}{M^2}} - 1 \right] - \frac{\delta_- M^2}{\mu_{d-}} \left[ \sqrt{1 + \frac{2\mu_{d-}\Phi}{M^2}} - 1 \right] - \delta_e \left( (1 + 3\beta - 3\beta\Phi + \beta\Phi^2) e^\Phi - (1 + 3\beta) \right) + \delta_p \left( \Phi - \frac{q+1}{4} \sigma_p \Phi^2 \right) \quad (15)$$

For a localized solution of equation (14) to exist, certain requirements must be satisfied [37]. It is clear that, for  $\phi = 0$ , the fixed point at the origin is unstable since  $V(\phi) = 0$ ,  $\frac{dV(\phi)}{d\phi} = 0$  and  $\frac{d^2V(\phi)}{d\phi^2} < 0$ . All the requirements are found to be met. Again,  $V(\phi) < 0$  must be satisfied between  $\phi = 0$  and  $\phi = \phi_m$ , where  $\phi_m$  represents the maximum (or minimum) value of  $\phi$  for which  $V(\phi_m) = 0$ .

The condition,  $\frac{d^2V(\phi)}{d\phi^2} < 0$  at  $\phi = 0$  gives the lower limit of Mach number ( $M_{min}$ ) as,

$$M_{min} = \sqrt{\frac{1 + \delta_+\mu_{d+} + \delta_-\mu_{d-}}{\delta_e(1 - \beta) + \frac{1}{2}\delta_p\sigma_p(q + 1)}}$$

The Mach number must satisfy  $M > M_{min}$  for the solitary waves to exist.

From equation (11) we observe that for  $n_i$  to be real we must have  $M^2 \geq 2\phi$ . Thus, the extreme value of  $\phi$  is,

$$\phi_m = \phi_0 = \frac{M^2}{2} \tag{16}$$

Substituting the extreme value of  $\phi$  from equation (16) in (15) we get the M upper limit as  $V(\phi) \geq 0$ , which gives,

$$M^2 - \frac{\delta_+M^2}{\mu_{d+}}[\sqrt{1 - \mu_{d+}} - 1] - \frac{\delta_-M^2}{\mu_{d-}}[\sqrt{1 + \mu_{d-}} - 1] - \delta_e \left[ \left( 1 + 3\beta - \frac{3}{2}\beta M^2 + \frac{1}{4}\beta M^4 \right) e^{\frac{M^2}{2}} - (1 + 3\beta) \right] + \delta_p \left[ \frac{M^2}{2} - \frac{q + 1}{16}\sigma_p M^4 \right] \geq 0$$

It is also crucial to investigate the profiles of solitary waves when their amplitudes are no longer arbitrary but small. To study small amplitude solitary waves, the Sagdeev Potential  $V(\phi)$  can be Taylor expanded about  $\phi=0$  up to a reasonable order of  $\phi$  so as to obtain a soliton solution from the energy integral equation.

Therefore, equation (14) can be reduced to,

$$\frac{1}{2} \left( \frac{d\phi}{d\xi} \right)^2 + A\phi^2 + B\phi^3 = 0, \tag{17}$$

where

$$A = \frac{\delta_+\mu_{d+}}{2M^2} + \frac{\delta_-\mu_{d-}}{2M^2} + \frac{\beta\delta_e}{2} - \frac{\delta_e}{2} + \frac{1}{2M^2} - \frac{\delta_p\sigma_p(q + 1)}{4}$$

$$B = \frac{\delta_+\mu_{d+}^2}{2M^4} - \frac{\delta_-\mu_{d-}^2}{2M^4} - \frac{\delta_e}{6} + \frac{1}{2M^4}$$

Integrating equation (17) and using the boundary conditions stated before, we obtain the soliton solution as,

$$\phi = \phi_m \operatorname{sech}^2 \left( \frac{\xi}{w} \right)$$

where,  $\phi_m = -\frac{A}{B}$  and  $w = \sqrt{-\frac{2}{A}}$  represents the amplitude and width of the soliton, respectively.

### 3. RESULTS AND DISCUSSION

The existence, structure, and characteristics of large-amplitude nonlinear waves, particularly solitary waves, can be analyzed by using the Sagdeev Potential method. Figure 1 shows the variation of the Sagdeev Potential for different values of the Mach number (M) and fixed  $\mu_{d+}=0.0000748$ ,  $\mu_{d-}=0.0000778$ ,  $\delta_+=0.38$ ,  $\delta_-=0.7$ ,  $\delta_e=0.8$ ,  $\beta=0.15$ ,  $\delta_p=0.12$ ,  $\sigma_p=0.2$ ,  $q=0.5$ . Figure 1 shows that as the Mach number (M) increases, depth of the Sagdeev potential well increases. Therefore, as M increases, the nonlinear effects in the plasma become more dominant over dispersive effects. This leads to an increase in the maximum amplitude of the electrostatic potential, which directly corresponds to a deeper and wider Sagdeev potential well.

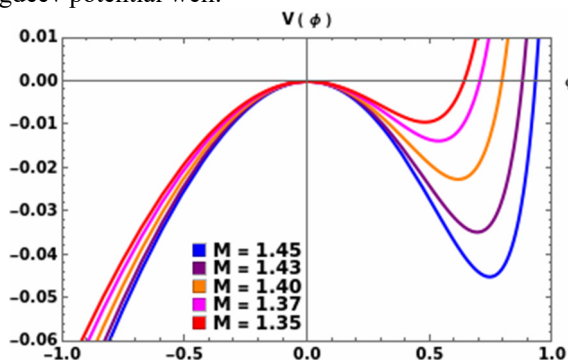


Figure 1. Variation of Sagdeev Potential  $V(\phi)$  with respect to  $\phi$  for different values of M

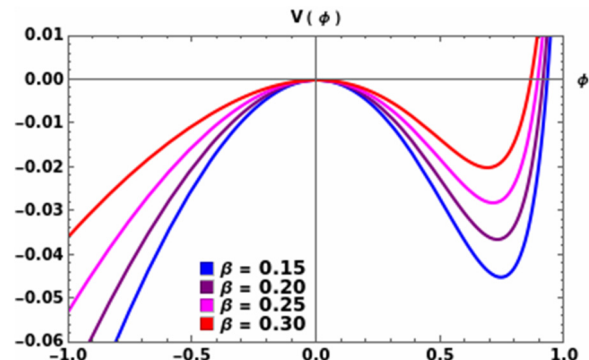


Figure 2. Variation of Sagdeev Potential  $V(\phi)$  with respect to  $\phi$  for different values of  $\beta$

Figure 2 shows the variation of the Sagdeev Potential for different values of non-thermal parameter  $\beta$  and fixed  $\mu_{d+}=0.0000748$ ,  $\mu_{d-}=0.0000778$ ,  $\delta_+=0.38$ ,  $\delta_-=0.7$ ,  $\delta_e=0.8$ ,  $\delta_p=0.12$ ,  $\sigma_p=0.2$ ,  $M=1.45$ ,  $q=0.5$ . Figure 2 shows that as the nonthermal electron parameter ( $\beta$ ) increases, the depth of the Sagdeev potential well decreases. Therefore, as the nonthermal parameter  $\beta$  increases, the increased population of high-energy electrons enhances the plasma's dispersion and weakens the nonlinear forces. This results in the formation of smaller-amplitude, broader solitary waves, represented by a shallower potential well.

Figure 3 shows the variation of the Sagdeev Potential for different values of the non-extensive parameter  $q$  and fixed  $\mu_{d+}=0.0000748$ ,  $\mu_{d-}=0.0000778$ ,  $\delta_+=0.38$ ,  $\delta_-=0.7$ ,  $\delta_e=0.8$ ,  $\beta=0.15$ ,  $\delta_p=0.12$ ,  $\sigma_p=0.2$ ,  $M=1.45$ . Figure 3 shows that as the non-extensive parameter ( $q$ ) increases, the depth of the Sagdeev potential well increases. Therefore, increasing  $q$  typically reduces the kinetic energy of the plasma species. This reduction makes energy exchange between the particles and the electric field easier, which enhances the amplitude of the electric field and effectively deepens the potential well. Figure 4 shows the variation of the Sagdeev Potential for different values of  $\sigma_p$  and fixed  $\mu_{d+}=0.0000748$ ,  $\mu_{d-}=0.0000778$ ,  $\delta_+=0.38$ ,  $\delta_-=0.7$ ,  $\delta_e=0.8$ ,  $\beta=0.15$ ,  $\delta_p=0.12$ ,  $M=1.45$ ,  $q=0.5$ . Figure 4 shows that as the electron to positron temperature ratio ( $\sigma_p$ ) increases, depth of the Sagdeev potential well increases. Therefore, higher temperatures allow electrons to behave more collectively. This collective interaction enhances the dispersion properties of the wave, and for a soliton to exist, the potential well must deepen to match the increased dispersion. As the electron temperature rises relative to the positron temperature, the thermal pressure of the electrons dominates, which can lead to a more significant separation of charge and a deeper potential well to balance the wave's kinetic energy.

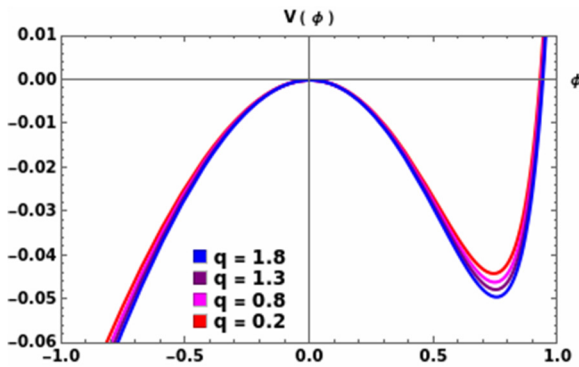


Figure 3. Variation of Sagdeev Potential  $V(\phi)$  with respect to  $\phi$  for different values of  $q$

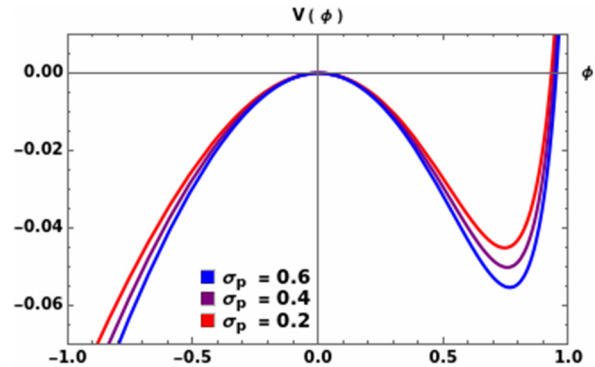


Figure 4. Variation of Sagdeev Potential  $V(\phi)$  with respect to  $\phi$  for different values of  $\sigma_p$

Figure 5 shows the variation of the Sagdeev Potential for different values of  $\delta_e$  and fixed  $\mu_{d+} = 0.0000748$ ,  $\mu_{d-} = 0.0000778$ ,  $\delta_-=0.7$ ,  $\beta=0.15$ ,  $\delta_p=0.12$ ,  $\sigma_p=0.2$ ,  $M=1.45$ ,  $q=0.5$ . Figure 5 shows that as electron to ion density ratio ( $\delta_e$ ) increases, depth of the Sagdeev potential well increases. An increase in  $\delta_e$  signifies a higher concentration of electrons relative to ions. In a moving wave frame, this leads to a stronger electric field and greater charge separation, which directly translates to a deeper potential well to maintain the wave structure. Figure 6 shows the variation of the Sagdeev Potential for different values of  $\delta_+$  and fixed  $\mu_{d+}=0.0000748$ ,  $\mu_{d-}=0.0000778$ ,  $\delta_-=0.7$ ,  $\beta=0.15$ ,  $\delta_p=0.12$ ,  $\sigma_p=0.2$ ,  $M=1.45$ ,  $q=0.5$ . Figure 6 shows that as charge density ratio of positively charged dust ( $\delta_+$ ) increases, depth of the Sagdeev potential well increases. We can say that, when the charge density ratio of positively charged dust ( $\delta_+$ ) increases, the depth of the Sagdeev potential well increases primarily due to the enhancement of the system's nonlinearity. As  $\delta_+$  increases, the contribution of the dust species to the Poisson equation becomes more significant. This shifts the balance between the dispersive and nonlinear effects in the plasma, typically leading to more robust (deeper and wider) potential well.

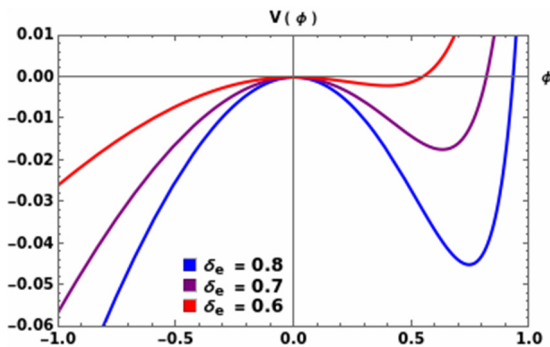


Figure 5. Variation of Sagdeev Potential  $V(\phi)$  with respect to  $\phi$  for different values of  $\delta_e$

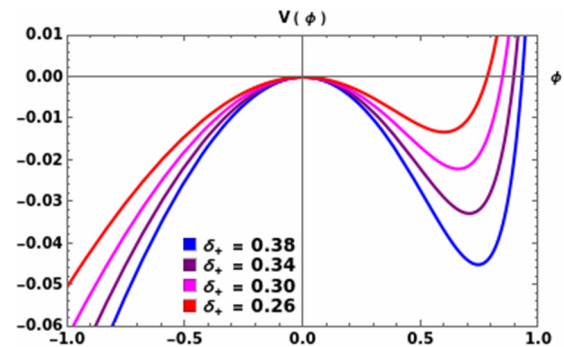


Figure 6. Variation of Sagdeev Potential  $V(\phi)$  with respect to  $\phi$  for different values of  $\delta_+$

Figure 7 shows the variation of the Sagdeev Potential for different values of  $\delta_-$  and fixed  $\mu_{d+}=0.0000748$ ,  $\mu_{d-}=0.0000778$ ,  $\delta_+=0.38$ ,  $\beta=0.15$ ,  $\delta_p=0.12$ ,  $\sigma_p=0.2$ ,  $M=1.45$ ,  $q=0.5$ . Figure 7 shows that as charge density ratio of

negatively charged dust ( $\delta_-$ ) increases, depth of the Sagdeev potential well decreases. Therefore, increasing  $\delta_-$  increases the overall inertia of the negative charge carrier in the plasma. This makes the system more sluggish, meaning it cannot reach the same high-potential amplitudes before the kinetic energy of the particles is exhausted, which manifests as a shallower potential well. Figure 8 shows the variation of the Sagdeev Potential for different values of  $\delta_p$  and fixed  $\mu_{d+}=0.0000748$ ,  $\mu_{d-}=0.0000778$ ,  $\delta_+=0.38$ ,  $\delta_-=0.7$ ,  $\beta=0.15$ ,  $\sigma_p=0.2$ ,  $M=1.45$ ,  $q=0.5$ . Figure 8 shows that as positron to ion density ratio ( $\delta_p$ ) increases, depth of the Sagdeev potential well increases. Since, positrons have the same mass as electrons but the opposite charge, they effectively neutralize some of the electron effects. This weakens the electrostatic restoring force that usually limits the growth of ion-acoustic waves. With a weaker restoring force, the plasma can support larger electric field gradients. Thus, the system becomes more nonlinear, allowing the solitary wave to acquire a larger maximum amplitude. In the Sagdeev potential framework, a larger amplitude translates directly to a deeper potential well.

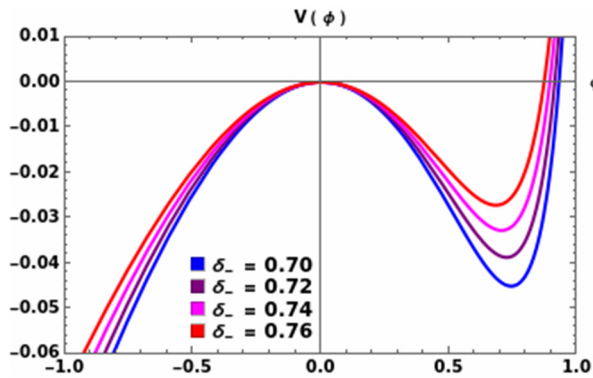


Figure 7. Variation of Sagdeev Potential  $V(\phi)$  with respect to  $\phi$  for different values of  $\delta_-$

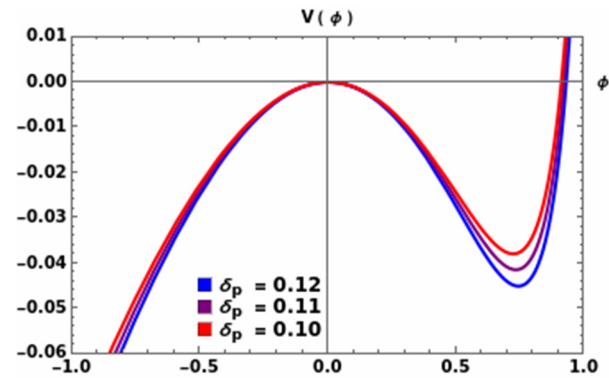


Figure 8. Variation of Sagdeev Potential  $V(\phi)$  with respect to  $\phi$  for different values of  $\delta_p$

Figure 9 shows the variation of  $M_{min}$  with respect to  $\beta$  for fixed  $\delta_+=0.38$ ,  $\mu_{d+}=0.0000748$ ,  $\delta_-=0.7$ ,  $\mu_{d-}=0.0000778$ ,  $\delta_e=0.8$ ,  $\delta_p=0.12$ ,  $\sigma_p=0.2$ ,  $q=0.8$ . We observe that as  $\beta$  increases,  $M_{min}$  gradually increases. Increase in  $\beta$  makes the plasma more rigid against the formation of solitary waves, requiring higher Mach number to initiate the nonlinear processes necessary for compressive solitons. Figure 10 shows the Variation of  $M_{min}$  with respect to  $q$  for fixed  $\delta_+=0.38$ ,  $\mu_{d+}=0.0000748$ ,  $\delta_-=0.7$ ,  $\mu_{d-}=0.0000778$ ,  $\delta_e=0.8$ ,  $\delta_p=0.12$ ,  $\sigma_p=0.2$ ,  $\beta=0.15$ . The figure shows that as  $q$  increases,  $M_{min}$  gradually decreases. Increasing  $q$  reduces the energetic tail of the positron distribution, lowering the plasma's acoustic speed and making it mathematically easier to reach the supersonic regime required for soliton existence.

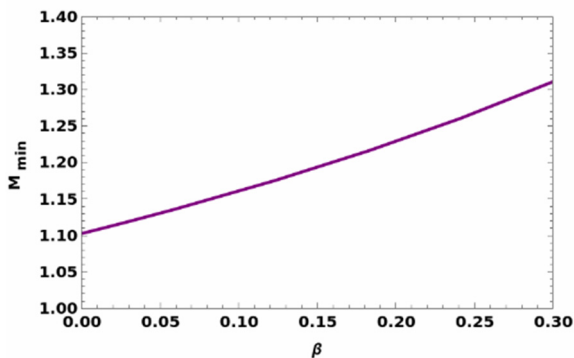


Figure 9. Variation of  $M_{min}$  with respect to  $\beta$

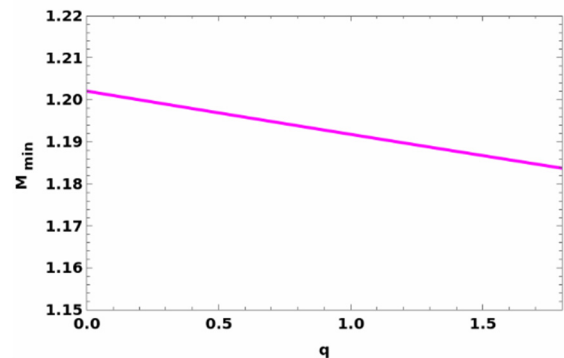


Figure 10. Variation of  $M_{min}$  with respect to  $q$

Figure 11 shows the Phase portrait for different values of  $M$  and fixed  $\delta_+=0.38$ ,  $\mu_{d+}=0.0000748$ ,  $\delta_-=0.7$ ,  $\mu_{d-}=0.0000778$ ,  $\delta_e=0.8$ ,  $\beta=0.15$ ,  $\delta_p=0.12$ ,  $\sigma_p=0.2$ ,  $q=0.5$ ,  $M=1.35$ . The closed loops and ending at the origin  $(0,0)$  represents homoclinic orbits. In plasma physics, these orbits correspond to solitary wave solutions where the potential and its gradient vanish at infinity. Because the loops exist on the positive side of the  $\phi$ -axis, these are compressive solitons. As the Mach number increases, amplitude increases. The point where the loop crosses the horizontal axis ( $\phi$ -axis) moves further to the right. This represents the peak amplitude of the soliton. Also, the maximum and minimum values of  $\frac{\partial\phi}{\partial\xi}$  (the height of the loop) increase, indicating that higher Mach numbers lead to solitons with steeper profiles. Figure 12 shows the Phase portrait for different values of  $\sigma_p$  and fixed  $\delta_+=0.38$ ,  $\mu_{d+}=0.0000748$ ,  $\delta_-=0.7$ ,  $\mu_{d-}=0.0000778$ ,  $\delta_e=0.8$ ,  $\beta=0.15$ ,  $\delta_p=0.12$ ,  $\sigma_p=0.5$ ,  $q=0.5$ ,  $M=1.45$ . As  $\sigma_p$  increases, the homoclinic orbits (the loops) expand further along the positive  $\phi$ -axis. This confirms that a higher temperature ratio leads to compressive solitons with larger amplitudes. The height of the loops increases as  $\sigma_p$  grows. This indicates that as the positrons become colder relative to the electrons (higher  $\sigma_p$ ), the resulting solitary wave becomes steeper (higher  $\frac{\partial\phi}{\partial\xi}$ ).

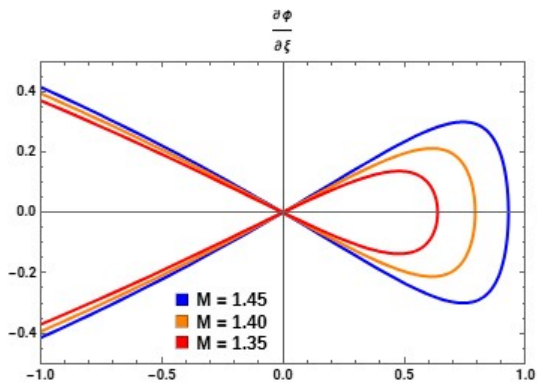


Figure 11. Phase portrait for different values of M

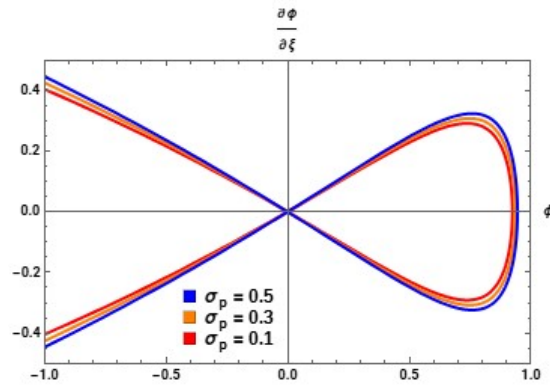


Figure 12. Phase portrait for different values of  $\sigma_p$

Figure 13 shows the variation of soliton profile with respect to  $\xi$  for different values of  $q$  and fixed  $\delta_+=0.6$ ,  $\mu_{d+}=0.0000748$ ,  $\delta_-=0.7$ ,  $\mu_{d-}=0.0000778$ ,  $\beta=0.25$ ,  $\delta_e=0.8$ ,  $\delta_p=0.53$ ,  $\sigma_p=0.5$ ,  $q=1.5$ ,  $M=1.15$ . We observe that as the value of  $q$  increases, the amplitude of soliton increases and the width decreases. Therefore, as  $q$  deviates from superextensive to subextensive regime, it enhances the energy of the solitons resulting the soliton structure to become taller and narrower. Figure 14 shows the variation of soliton profile with respect to  $\xi$  for different values of  $\beta$  and fixed  $\delta_+=0.6$ ,  $\mu_{d+}=0.0000748$ ,  $\delta_-=0.7$ ,  $\mu_{d-}=0.0000778$ ,  $\beta=0.15$ ,  $\delta_e=0.8$ ,  $\delta_p=0.53$ ,  $\sigma_p=0.5$ ,  $q=0.8$ ,  $M=1.15$ . We observe that as the value of  $\beta$  increases the amplitude of soliton decreases and the width increases. Therefore, the effect of the non-extensive parameter  $q$  and the nonthermal parameter  $\beta$  are opposite on the soliton profile for small amplitude solitons. This is same as the effect of  $q$  and  $\beta$  on large amplitude solitons.

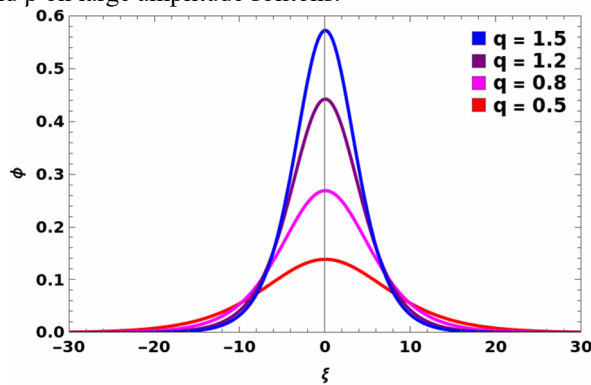


Figure 13. Variation of soliton profile with respect to  $\xi$  for different values of  $q$

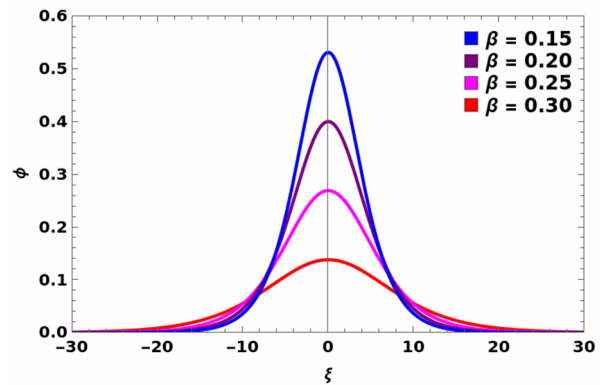


Figure 14. Variation of soliton profile with respect to  $\xi$  for different values of  $\beta$

Figure 15 shows the variation of soliton profile with respect to  $\xi$  for different values of  $\sigma_p$  and fixed  $\delta_+=0.6$ ,  $\mu_{d+}=0.0000748$ ,  $\delta_-=0.7$ ,  $\mu_{d-}=0.0000778$ ,  $\beta=0.15$ ,  $\delta_e=0.8$ ,  $\delta_p=0.53$ ,  $\sigma_p=0.3$ ,  $q=0.8$ ,  $M=1.15$ . We observe that, as the value of  $\sigma_p$  increases, the amplitude of soliton increases and the width decreases. Therefore, as the electrons become relatively hotter than the positrons, the solitons become taller and narrower. This indicates increase in energy of soliton for increasing values of  $\sigma_p$ .

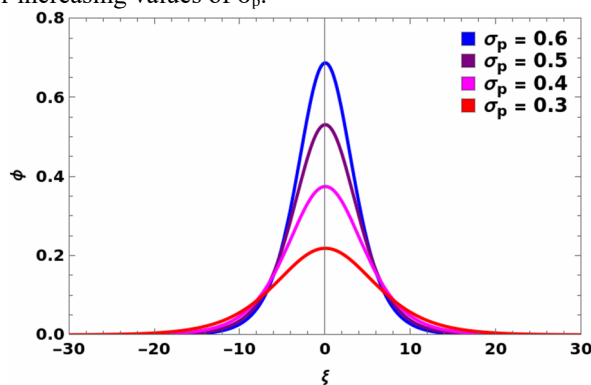


Figure 15. Variation of soliton profile with respect to  $\xi$  for different values of  $\sigma_p$

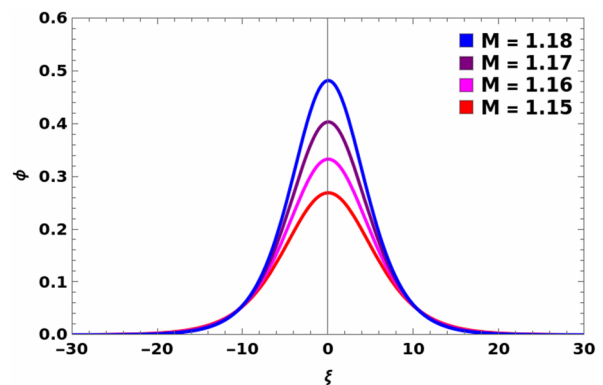


Figure 16. Variation of soliton profile with respect to  $\xi$  for different values of M

Figure 16 shows the variation of Soliton profile with respect to  $\xi$  for different values of M and fixed  $\delta_+=0.6$ ,  $\mu_{d+}=0.0000748$ ,  $\delta_-=0.7$ ,  $\mu_{d-}=0.0000778$ ,  $\beta=0.25$ ,  $\delta_e=0.8$ ,  $\delta_p=0.53$ ,  $\sigma_p=0.5$ ,  $q=0.8$ ,  $M=1.18$ . We observe that as

the value of  $M$  increases, the amplitude of soliton also increases and the width decreases. Therefore, as  $M$  increases, the nonlinear effects in the plasma become more dominant over dispersive effects. We observe that the effects of the electron to positron temperature ratio  $\sigma_p$  and the Mach number  $M$  is same on the soliton profile for small amplitude solitons. This is same as the effect of  $\sigma_p$  and  $M$  on large amplitude solitons.

#### 4. CONCLUSIONS

In the study of solitons in an unmagnetized dusty plasma composed of cold ions, negatively charged dust grains, positively charged dust grains, non-thermal electrons and non-extensive positrons, we have found the existence of compressive solitons. The solitons are found to exist in our plasma model for a supersonic regime ( $M > 1$ ). The compressive solitons are found to be influenced by the non-extensive parameter ( $q$ ), the non-thermal parameter ( $\beta$ ), charge density ratio of positively charged dust ( $\delta_+$ ), charge density ratio of negatively charged dust ( $\delta_-$ ), positron to ion density ratio ( $\delta_p$ ), electron to ion density ratio ( $\delta_e$ ), electron to positron temperature ratio ( $\sigma_p$ ) and the Mach number ( $M$ ). The increase in the depth of the Sagdeev potential well represents increase in the amplitude of the solitons. The amplitude of the compressive solitons is found to increase for increasing values of  $M$ ,  $\delta_p$ ,  $\delta_+$ ,  $\delta_e$ ,  $q$  and  $\sigma_p$ ; however, amplitude of the compressive solitons found to decrease for increasing values of  $\delta_-$  and  $\beta$ . The dual nature of the dust population plays a critical role in wave dynamics; while positively charged dust ( $\delta_+$ ) enhances the nonlinear potential, the negative dust component ( $\delta_-$ ) provides significant inertia that acts to suppress the growth of compressive structures. Similarly, the statistical deviation from Maxwellian behaviour shows that non-extensive positrons favour soliton growth, whereas non-thermal electrons act as a dampening mechanism, illustrating the high sensitivity of the system to the specific energy distribution of its lighter species. The influence of non-thermal electrons and non-extensive positrons on ion-acoustic solitary waves in a multi-component plasma was investigated in [36]. Variation of Sagdeev Potential was investigated in [36] for  $0.4 \leq q \leq 2.9$ . However, in our study, Sagdeev Potential shows significant variations for  $0.2 \leq q \leq 1.8$ . This change in range in our plasma model is because of involvement of dust components, which makes the effect of the non-extensive parameter ( $q$ ) towards Sagdeev potential more sensitive. These effects of the parameters can have influence on understanding the nonlinear solitary structures present in astrophysical environment.

#### ORCID

✉ Satyendra Nath Barman, <https://orcid.org/0000-0003-1136-8364>; ✉ Kingkar Talukdar, <https://orcid.org/0009-0007-5419-134X>

#### REFERENCES

- [1] S. Dalui, and A. Bandyopadhyay, "Effect of Landau damping on ion acoustic solitary waves in a collisionless unmagnetized plasma consisting of nonthermal and isothermal electrons," *Indian J Phys*, **95**, 367–381 (2021). <https://doi.org/10.1007/s12648-020-01731-5>
- [2] A.S.M. Moinuddin, M. S. Alam, and M.R. Talukder, "Head-on collision of ion-acoustic waves in multi-component unmagnetized plasmas," *Waves in Random and Complex Media*, **32**(6), 2657-2676 (2022). <https://doi.org/10.1080/17455030.2020.1859163>
- [3] M.G. Hafez, M.R. Talukder, and M.H. Ali, "Nonlinear propagation of weakly relativistic ion-acoustic waves in electron–positron–ion plasma," *Pramana*, **87**(5), 70 (2016). <https://doi.org/10.1007/s12043-016-1275-x>
- [4] P. Halder, A. Bandyopadhyay, and S. Sardar, "Arbitrary Amplitude Dust–Ion Acoustic Solitary Structures in Five Components Unmagnetized Plasma," *Plasma Phys. Rep.* **49**, 467–483 (2023) <https://doi.org/10.1134/S1063780X22601225>
- [5] A.E. Dubinov and D.Y. Kolotkov, "Ion-acoustic supersolitons in plasma," *Plasma Phys. Rep.* **38**, 909–912 (2012). <https://doi.org/10.1134/S1063780X12100054>
- [6] M.N. Islam, M.G. Hafez, and U.K. Deb, "Heavy Ion-Acoustic Soliton and Dressed Soliton in an Unmagnetized Weakly and Strongly Coupled Plasma," *Braz. J. Phys.* **52**, 158 (2022). <https://doi.org/10.1007/s13538-022-01141-4>
- [7] G.S. Lakhina, A.P. Kakad, S.V. Singh, and F. Verheest, "Ion- and electron-acoustic solitons in two-electron temperature space plasmas," *Phys. Plasmas*, **15**(6), 062903 (2008). <https://doi.org/10.1063/1.2930469>
- [8] M.G. Hafez, and M.R. Talukder, "Ion acoustic solitary waves in plasmas with nonextensive electrons, Boltzmann positrons and relativistic thermal ions," *Astrophys. Space Sci.* **359**, 27 (2015). <https://doi.org/10.1007/s10509-015-2480-7>
- [9] M. O. Rahman, M. G. Hafez, S. Barua, and M. A. Kausar, "Ion acoustic solitons and periodic waves with dynamical features around the supercritical values in relativistic unmagnetized plasmas," *Physica Scripta*, **100**(2), 025201 (2025). <https://doi.org/10.1088/1402-4896/ada20b>
- [10] U. Imon, and M. S. Alam, "Consequence of head-on collision of ion acoustic waves in unmagnetized plasmas having generalized ( $r, q$ ) distributed electrons and positrons," *Waves in Random and Complex Media*, 1–28. (2023). <https://doi.org/10.1080/17455030.2023.2280910>
- [11] H. Ur-Rehman and S. Mahmood, "Higher order contribution to ion-acoustic Korteweg–de Vries (KdV) soliton in unmagnetized quantum plasmas with arbitrary degeneracy of electrons," *Physica Scripta*, **99**(7), 075608. (2024). <https://doi.org/10.1088/1402-4896/ad52f8>
- [12] H. Alinejad, "Non-linear localized ion-acoustic waves in electron–positron–ion plasmas with trapped and non-thermal electrons," *Astrophys. Space Sci.* **325**, 209–215 (2010). <https://doi.org/10.1007/s10509-009-0177-5>
- [13] M.G. Hafez, M.R. Talukder and R. Sakthivel, "Ion acoustic solitary waves in plasmas with nonextensive distributed electrons, positrons and relativistic thermal ions," *Indian J Phys*, **90**, 603–611 (2016). <https://doi.org/10.1007/s12648-015-0782-9>
- [14] T. Kaladze, S. Mahmood and H. Ur-Rehman, "Acoustic nonlinear periodic (cnoidal) waves and solitons in pair-ion plasmas," *Physica Scripta*, **86**(3), 035506. (2012). <https://doi.org/10.1088/0031-8949/86/03/035506>
- [15] P. Mandal, T.K. Maji, U.K. Samanta and M. K. Ghorui, "Head-on collision of ion-acoustic KP solitons in unmagnetized e-p-i plasma," *Indian J. Phys.* **99**, 4833–4843 (2025). <https://doi.org/10.1007/s12648-025-03631-y>
- [16] M.M. Alam and M.S. Alam, "Study of Time-Fractional Dust Ion Acoustic Waves Propagation in Collisionless Unmagnetized Dusty Plasmas," *Braz. J. Phys.* **54**, 192 (2024) <https://doi.org/10.1007/s13538-024-01562-3>

- [17] M. Khalid, A. Khan, M. Khan, F. Hadi, and A. Rahman, "Dust Ion Acoustic Solitary Waves in Unmagnetized Plasma with Kaniadakis Distributed Electrons," *Braz J Phys*, **51**, 60–65 (2021). <https://doi.org/10.1007/s13538-020-00807-1>
- [18] R. Bharuthram and P.K. Shukla, "Large amplitude ion-acoustic solitons in a dusty plasma," *Planetary and Space Science*, **40**(7), 973-977 (1992) [https://doi.org/10.1016/0032-0633\(92\)90137-D](https://doi.org/10.1016/0032-0633(92)90137-D).
- [19] R.S. Tiwari, and M.K. Mishra, "Ion-acoustic dressed solitons in a dusty plasma," *Phys. Plasmas* **13**(6), 062112 (2006) <https://doi.org/10.1063/1.2216936>
- [20] S.K. El-Labany, and W.F. El-Taibany, "Effect of dust-charge variation on dust acoustic solitary waves in a dusty plasma with trapped electrons," *Journal of plasma physics*, **70**(1), 69-87 (2004). <https://doi.org/10.1017/S0022377803002460>
- [21] S. Das, "Weak Relativistic Effect in the Formation of Ion-Acoustic Solitary Waves in Dusty Plasma," *IEEE Transactions on Plasma Science*, **50**, 2225-2229 (2022). <https://doi.org/10.1109/TPS.2022.3181149>
- [22] M. Shahmansouri, and M. Tribeche, "Large amplitude dust ion acoustic solitons and double layers in dusty plasmas with ion streaming and high-energy tail electron distribution," *Commun. Theor. Phys*, **61**, 377 (2014). <https://doi.org/10.1088/0253-6102/61/3/18>
- [23] S. Das, "Propagation of dust ion acoustic solitary waves in dusty plasma with Boltzmann electrons," *J. Phys.: Conf. Ser.* **1290**, 012025 (2019). <https://doi.org/10.1088/1742-6596/1290/1/012025>
- [24] R. Tomar, H.K. Malik, and R.P. Dahiya, "Reflection of ion acoustic solitary waves in a dusty plasma with variable charge dust," *J. Theor. Appl. Phys.* **8**, 126 (2014). <https://doi.org/10.1007/s40094-014-0126-8>
- [25] M. Das, B. Madhukalya, and R. Das, "Ion acoustic solitary waves in multicomponent plasmas: influence of ion drift velocity and nonthermal electrons," *Heat Transfer*, **53**, 2062-2072 (2024). <https://doi.org/10.1002/htj.23027>
- [26] S.V. Singh, and G.S. Lakhina, "Electron acoustic solitary waves with non-thermal distribution of electrons," *Nonlinear Processes in Geophysics*, **11**(2), 275-279 (2004). <https://doi.org/10.5194/npg-11-275-2004>
- [27] T.S. Gill, H. Kaur, and N.S. Saini, "Small amplitude electron-acoustic solitary waves in a plasma with nonthermal electrons," *Chaos, Solitons & Fractals*, **30**(4), 1020-1024 (2006). <https://doi.org/10.1016/j.chaos.2005.09.070>
- [28] R. Sabry, W.M. Moslem, and P.K. Shukla, "Fully nonlinear ion-acoustic solitary waves in a plasma with positive-negative ions and nonthermal electrons," *Physics of Plasmas*, **16**(3), (2009) <https://doi.org/10.1063/1.3088005>
- [29] H.A. Alyousef, S.N. Naem, M. Irshad, Ata-ur-Rahman, Sherif M.E. Ismaeel, and S.A. El-Tantawy, "The impact of electron beams on the arbitrary amplitude electron-acoustic solitons in a nonthermal plasma," *Physics of Fluids*, **36**(1), 015139 (2024). <https://doi.org/10.1063/5.0181144>
- [30] S.V. Singh, and G.S. Lakhina, "Ion-acoustic supersolitons in the presence of non-thermal electrons," *Communications in Nonlinear Science and Numerical Simulation*, **23**(1-3), 274-281 (2015). <https://doi.org/10.1016/j.cnsns.2014.11.017>
- [31] S.K. Maharaj, and R. Bharuthram, "Non-thermal effects of electrons on stopbands of fast ion-acoustic solitons," *Physics of Plasmas*, **24**(2), (2017) <https://doi.org/10.1063/1.4975317>
- [32] U.N. Ghosh, A. Saha, N. Pal, and P. Chatterjee, "Dynamic structures of nonlinear ion acoustic waves in a nonextensive electron-positron-ion plasma," *J. Theor. Appl. Phys.* **9**, 321–329 (2015). <https://doi.org/10.1007/s40094-015-0192-6>
- [33] R. Khanam, and S.N. Barman, "The Formation of Ion-Acoustic Solitary Waves in a Plasma Having Nonextensive Electrons and Positrons," *East European Journal of Physics*, (4), 518-525 (2024). <https://doi.org/10.26565/2312-4334-2024-4-61>
- [34] U.N. Ghosh, D.K. Ghosh, P. Chatterjee, M. Bacha, and M. Tribeche, "Nonplanar ion-acoustic Gardner solitons in a pair-ion plasma with nonextensive electrons and positrons," *Astrophys. Space. Sci.* **343**, 265–272 (2013). <https://doi.org/10.1007/s10509-012-1221-4>
- [35] M.A. Khaled, "On the head-on collision between two ion acoustic solitary waves in a weakly relativistic plasma containing nonextensive electrons and positrons," *Astrophys. Space. Sci.* **350**, 607–614 (2014). <https://doi.org/10.1007/s10509-014-1790-5>
- [36] M. Nasir, L. Ameen, B. Asghar, N. Beemkumar, V. Jain, S. Imtiaz, M.F. Ullah, *et al.*, "Influence of non-thermal electrons and non-extensive positrons on ion acoustic solitary waves in multi-component plasmas," *International Communications in Heat and Mass Transfer*, **170**, 110026 (2026). <https://doi.org/10.1016/j.icheatmasstransfer.2025.110026>
- [37] A. Mushtaq, M. Nasir Khattak, Z. Ahmad, and A. Qamar, "Dust ion acoustic soliton in pair-ion plasmas with non-isothermal electrons," *Physics of Plasmas*, **19**(4), 042304 (2012). <https://doi.org/10.1063/1.3696061>
- [38] A. Renyi, "On a new axiomatic theory of probability," *Acta Math. Hung.* **6**, 285-335 (1955). <https://doi.org/10.1007/bf02024393>
- [39] C. Tsallis, "Possible generalization of Boltzmann-Gibbs statistics," *Journal of statistical physics*, **52**(1), 479-487 (1988). <https://doi.org/10.1007/BF01016429>
- [40] M.N. Khattak, A. Mushtaq, and Z. Ehsan, "Electrostatic baryonic solitary waves in ambiplasma with nonextensive leptons," *Chinese Journal of Physics*, **54**(4), 503–514 (2016). <https://doi.org/10.1016/j.cjph.2016.06.011>

## ВПЛИВ НЕТЕПЛОВИХ ЕЛЕКТРОНІВ ТА НЕЕКСТЕНСИВНИХ ПОЗИТРОНІВ НА ОДИНОЧНІ ХВИЛІ В БАГАТОКОМПОНЕНТНІЙ ПИЛІВІЙ ПЛАЗМІ

Сатьєндра Натх Барман<sup>1</sup>, Кінгкар Талукдар<sup>2</sup>

<sup>1</sup>Коледж В. Боруа, Гувахаті 781007, Ассам, Індія

<sup>2</sup>Кафедра математики, Університет Гаухаті, Гувахаті 781014, Ассам, Індія

У цьому дослідженні ми вивчали існування та характеристики солітонів у немагнітній запиленій плазмі, що складається з холодних іонів, негативно заряджених пилових частинок, позитивно заряджених пилових частинок, нетеплових електронів та неекстенсивних позитронів. Властивості солітонів зазвичай вивчаються за допомогою методу редукційних збурень та методу потенціалу Сагдєєва. Ми вивели інтегральне рівняння енергії, використовуючи метод потенціалу Сагдєєва. Ми також обговорили зміну потенціалу Сагдєєва для різних значень параметрів, що беруть участь у нашій моделі плазми. Неекстенсивний параметр ( $q$ ), нетепловий параметр ( $\beta$ ), коефіцієнт густини заряду позитивно зарядженого пилу ( $\delta_+$ ), коефіцієнт густини заряду негативно зарядженого пилу ( $\delta_-$ ), коефіцієнт густини позитронів до іонів ( $\delta_p$ ), коефіцієнт густини електронів до іонів ( $\delta_e$ ), коефіцієнт температури електронів до позитронів ( $\sigma_p$ ) та число Маха ( $M$ ) впливають на амплітуду солітонів. Наше дослідження показує, що нетермальність електронів та неекстенсивність позитронів суттєво змінюють характеристики солітонів. Результати нашого дослідження можуть бути корисними для вивчення плазми в космічних середовищах, таких як кометні хвости та міжзор'яні хмари.

**Ключові слова:** нетепловий режим; одиночні хвилі; потенціал Сагдєєва; інтеграл енергії; пилова плазма